

Chapter 6A) Formulation
Development: DPK-060
Nano-lipid Constructs

Dermal Delivery of Protein/Peptide Based Antimicrobial to
Treat Secondary Infection in Psoriasis and Eczema

6A.1 Introduction

The objective of our present investigation was to develop and characterize NLCs of DPK-060 for dermal delivery. These NPs can control the release of the therapeutic agent and ensure delivery in the desired manner and have been widely reported in the literature [1-3]. Several molecules (hydrophobic/ hydrophilic) have been encapsulated in the NLCs by the melt-emulsification method followed by high-pressure homogenization. Hence, this method was selected to prepare DPK-060 loaded NLCs [4-7]. A systematic QbD approach employing statistical design of experiments was utilized to exhaustively assess the impact of material attributes and process parameters on the critical formulation attributes [8, 9].

6A.2 Materials and Instruments

6A.2.1 Materials

Table 6A.1 List of materials

Materials & Reagents	Manufacturers
DPK-060	S-Biochem, Kerala, India (Custom synthesis)
Methanol (A.R. & HPLC Grade)	Spectrochem Pvt. Ltd., Mumbai
Miglyol- 840	Gattefosse, Mumbai
Compritol 888 ATO	Gattefosse, Mumbai
Tween 80	MP Biomedicals Pvt. Ltd., Mumbai
Egg lecithin	Lipoid GmbH, Germany
Distilled water	Prepared In-house

6A.2.2 Instruments

Table 6A.2 List of instruments

Equipment	Manufacturer
Digital Weighing Balance	Shimadzu, Japan
RP-HPLC with UV Detector (gradient)	Agilent OpenLab CDS EZChrom, India
Vortex mixer	Spinix, Japan
Magnetic stirrer	Remi equipments Pvt Ltd., India

pH meter	Lab India Pvt. Ltd, Mumbai
Filtration assembly	Durga scientific Pvt. Ltd., Baroda
Centrifuge	Remi equipments Pvt. Ltd., India
Distillation assembly	Durga glassware, India
High Pressure Homogenizer	Avestin, India
Particle size analyzer (Nano-ZS)	Malvern Instrument, UK
Scanning electron microscope	EVO-18, Zeiss, Germany

6A.3 Methodology

6A.3.1 Preparation of DPK-060 loaded nano-lipid constructs

DPK-060 loaded NLCs were formulated by melt-emulsification method [4-7]. Briefly, Compritol 888 ATO and Miglyol- 840 was taken in 7:3 ratios along with the egg lecithin. Subsequently, the aqueous phase was prepared by dissolving the Tween 80 in 5 ml of 20 mM acetate buffer pH 5.5. Both of these phases were maintained at 75°C, and DPK-060 (1% w/w) was added into the melted lipid matrix, followed by addition of the aqueous phase to the lipid phase drop by drop under the continuous stirring at 700 rpm using a magnetic stirrer at room temperature to get a homogeneous emulsion. The surfactant ratio of 2:1 (Tween 80: egg lecithin) was used to prepare DPK-060 loaded NLCs due to the higher emulsification ability. The resultant NLC particles were then subjected to HPH (10000 psi * 10 cycles) for size reduction. Subsequently, this NLC dispersion was centrifuged at 18,000 rpm (4 °C for 30 min) to separate the free drug and NLCs.

6A.3.2 QbD approach for the formulation development

Before developing any formulation, there is a strong need to identify formulation variables, process variables, and environmental variables expected to affect the product characteristics. Ishikawa diagram (Fig. 6A.1) was used to determine all the probable variables, i.e., formulation, process, and environment variables associated with the development of DPK-060 loaded NLCs by melt-emulsification method (Table 6A.3).

Table 6A.3 List of variables mainly affecting DPK-060 NLC formulation

Formulation variables	Process variables	Environment variables
Drug (DPK-060)	Mixing of components	Temperature
Concentration of Lipids	The volume of organic phase	
Drug: lipid ratio	Stirring speed	
Surfactant concentration	Stirring time	
Lipid phase volume	Rate of addition of organic phase	
pH of solution	Bead size	

Quality Target Product Profile (QTPP)

For the development of an accurate, precise, and reproducible manufacturing method as a quality target product profile, the following attributes were considered that will ensure desired product quality in all aspects of QTPP:

- ✓ % Entrapment Efficiency and % drug loading: high
- ✓ Particle Size: 200-300 nm
- ✓ Drug release from nano-lipid constructs: NLT 60% in 6 hr

6A.3.2.1 Optimization of Formulation by Box-Behnken Design (BBD)

The values of the selected variable for BBD i.e., independent variables and dependent variables (response parameters) are shown in Table 6A.4.

Table 6A.4 Selected values of variables for BBD

Variables	Levels (-1, 0, 1)
Independent variables	
A: Lipid concentration (% w/w) (X1)	2,3,4
B: Surfactant concentration (% w/w) (X2)	5,10,15
C: Homogenization cycles (No.) (X3)	5,10,15
Constant parameters	
Rate of organic phase addition (ml/min)	1 ml/min
The volume of organic solvent (ml)	2 ml
Stirring time (min)	30 min
Stirring speed (rpm)	700 rpm

Homogenization pressure (psi)	10000 psi
Temperature (°c)	25-40°C (room temp.)
Dependent variables (response parameters)	
% Drug entrapment (%) (Y1)	
Particle size (nm) (Y2)	

The selection of critical formulation variables was made according to the results obtained in the preliminary investigation. A BBD design matrix was generated using Stat-Ease Design-Expert Software 13.0. Total 17 experimental runs were obtained from the software. All the batches of DPK-060 nano-lipid constructs were prepared according to the design matrix while keeping all other process variables constant. % Drug entrapment and particle size of the formulated DPK-060 nano-lipid constructs were taken as response parameters (CQA).

6A.3.2.2 Particle size

The particle size of DPK-060 loaded NLCs were determined using Nano-ZS Zetasizer, Malvern Instruments Ltd., UK. Briefly, DPK-060 NLC dispersion was diluted 10 times with filtered distilled water and transferred to disposable sizing cuvette/folded capillary cells to measure particle size.

6A.3.2.3 % Drug entrapment

To determine the % drug entrapment, DPK-060 NLC dispersion was centrifuged at 18,000 rpm for 30 min at 4 °C. The sedimented NLC fraction was dissolved in water: methanol (2:8) mixture and analyzed by the developed HPLC method (chapter 3). To ensure the mass balance of the drug, the supernatant was also analyzed for the free DPK-060 content using the HPLC method at 220 nm. % Drug loading was quantified by using the mass (weight) of the centrifuged pellet of NLCs. Following equations were used to calculate the % drug entrapment and % drug loading: [10]

$$\% \text{ Drug entrapment} = \frac{\text{Amount of entrapped drug}}{\text{Total drug added}} \times 100$$

$$\% \text{ Drug loading} = \frac{\text{Drug loaded (mg)}}{\text{Total weight of NLCs (mg)}} \times 100$$

6A.3.2.4 Preparation of gel for DPK-060 and DPK-060 nano-lipid constructs

The gel-based formulation was developed and loaded with DPK-060 (1%w/v) and optimized DPK-060 NLCs (having 1%w/v DPK-060 concentration) to improve the viscosity of the formulation for better skin retention. Briefly, the weighed quantity of Carbopol 934P (1.2%w/v) was mixed and dispersed in DPK-060 NLC dispersion (1%w/v) using an overhead stirrer at 2000 rpm for 1 h. After hydration, the mixture of methylparaben (0.2%w/v) and propylparaben (0.02%w/v) in propylene glycol (4%w/v) was added with continuous stirring. The pH of the formulation was adjusted to ~6.5 by dropwise addition of 10% v/v Sodium hydroxide solution. The detailed formulation composition is showed in Table 6A.5.

Table 6A.5 Formulation components with their concentration used in the preparation of DPK-060 NLC gel

Formulation components	Concentration
DPK-060/DPK-060 NLCs	1% w/v
Carbopol 934P	1.20% w/v
Propylene glycol	4% w/v
Methyl paraben and propyl paraben	0.2 and 0.02 %w/v
Sodium hydroxide solution (10%v/v)	...qs...to pH 6.5

6A.3.3 Characterization of optimized DPK-060 nano-lipid constructs and NLC gel

6A.3.3.1 Zeta potential

The zeta potential of DPK-060 NLC dispersion was measured using a Nano-ZS zeta sizer equipped with a 5-mV He-Ne laser. Briefly, DPK-060 NLC dispersion was diluted 10 times with filtered distilled water and transferred to disposable folded capillary cells. An average of 30 measurements of each sample was used to get average zeta potential.

6A.3.3.2 Shape and surface morphology

The optimized DPK-060 NLCs were examined for shape and surface characteristics using SEM. Briefly, the sample was gold-coated using a sputter coater

(Emitech) for 4 min at 10 mA current. After that, sample was attached to the aluminium stubs and then observed using an accelerating voltage of 15.00 kV at different magnifications.

6A.3.3.3 Viscosity of DPK-060 gel

The viscosity of free DPK-060 gel and DPK-060 NLC gel was determined using cone and plate rheometer (Bohlin C-VOR, Malvern Instruments Ltd., UK) at $25\pm 1^\circ\text{C}$. In brief, 200 mg of the sample was placed on the sample holder. After that, the spindle was lowered and kept for equilibrium for 5 min having a plate width of 20 mm and a cone angle of 4° . Subsequently, the spindle was rotated at a shear rate of 10/s, and viscosity (Pa.S) observed was reported (n=3) [11].

6A.3.3.4 Spreadability of DPK-060 gel

The spreadability of free DPK-060 gel and DPK-060 NLC gel was evaluated by the previously reported method [12]. Briefly, 500 mg of sample was placed on a pre-marked circle with a 1 cm diameter on the glass plate over which a second glass plate was positioned. Subsequently, 500 g weight was applied on the upper glass plate for 5 min, and any change in diameter was reported (n=3).

6A.3.3.5 pH of DPK-060 gel

The pH of free DPK-060 gel and DPK-060 NLC gel was measured using a digital pH meter (Lab India Pvt. Ltd, Mumbai).

6A.3.3.6 Assay of DPK-060 gel

The DPK-060 content from the free DPK-060 gel and DPK-060 NLC gel was determined by dissolving the 100 mg of sample in the PBS pH 7.4: methanol mixture (8:2 ratio). The amount of DPK-060 was quantified by the developed gradient HPLC method.

6A.4 Results and Discussion

6A.4.1 Preparation and optimization of DPK-060 nano-lipid constructs

6A.4.1.1 Establishment of QTPP

The variables linked with the development of DPK-060 loaded NLCs by reverse-phase evaporation technique were identified into Process, Formulation, and Environment. Ishikawa diagram (Fig. 6A.1) was used to determine the variables linked with the development of DPK-060 loaded NLCs.

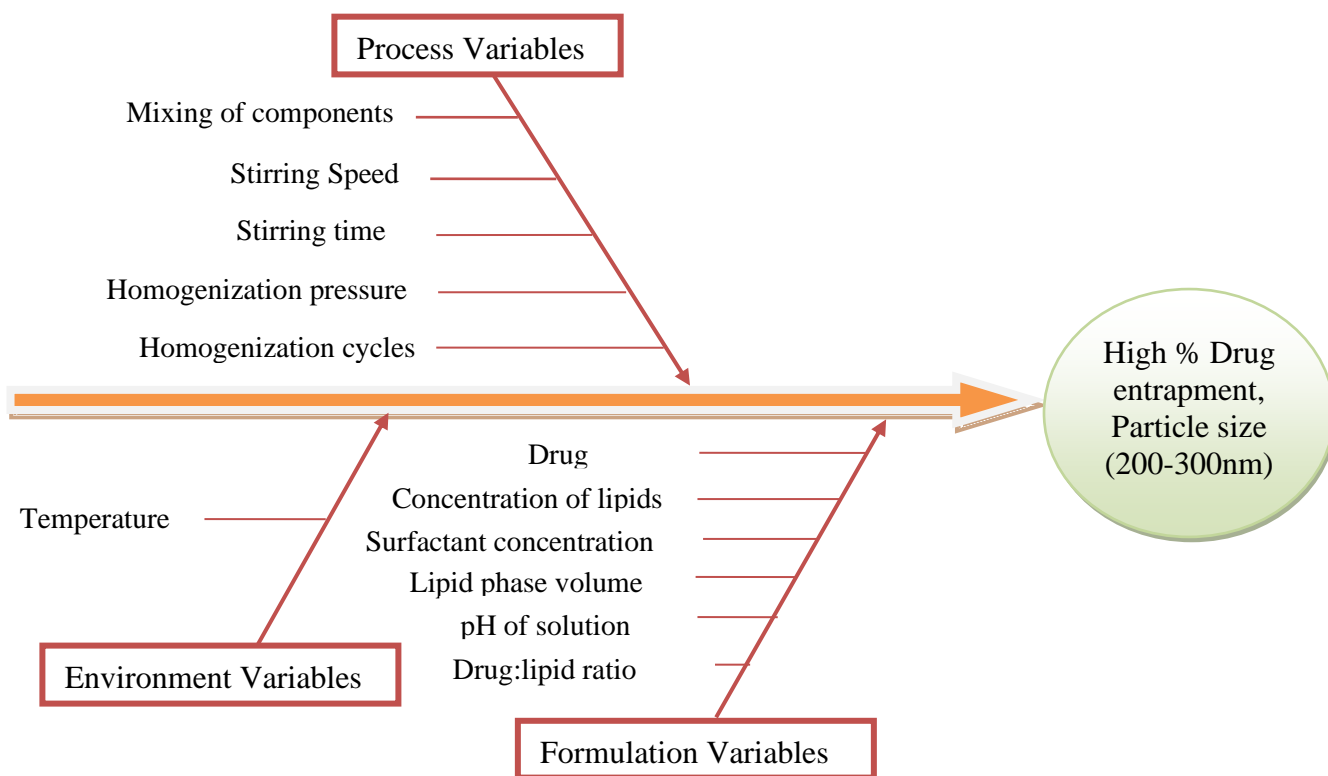


Fig. 6A.1 Ishikawa diagram showing probable variables that may influence CQA

6A.4.1.2 Formulation optimization by Box-Behnken Design

Based on the preliminary investigation, three CMA were identified, and their relationship with CQA was exhaustively investigated using Box-Behnken Design. A randomized matrix of 17 runs was generated by Design-Expert software and presented in Table 6A.6.

Table 6A.6 Randomized BBD design matrix generated by Design-Expert software

Run	Dependent variables			Independent variables	
	A: Lipid concentration (% w/w)	B: Surfactant concentration (% w/w)	C: Homogenization cycles (No.)	% Drug entrapment	Particle size (nm)
1	3	10	15	67.42	126.8
2	3	10	5	70.77	143.2
3	4	10	10	84.14	123.5
4	4	5	5	83.91	151.8
5	5	10	15	81.1	166.8
6	4	15	15	79.32	115.4
7	4	5	15	78.01	120.8
8	4	10	10	85.12	129.8
9	5	10	5	87.54	205.6
10	4	10	10	83.78	127.1
11	4	15	5	84.79	145.4
12	3	15	10	68.26	132.6
13	3	5	10	68.47	137.8
14	5	5	10	85.55	181.3
15	4	10	10	84.73	125.6
16	5	15	10	87.15	170.1
17	4	10	10	85.07	128.2

6A.4.1.3 Effect analysis of critical variables on responses

6A.4.1.3.1 Influence of investigated parameters on % Drug entrapment

A) Statistical Analysis for % Drug entrapment

The statistical analysis of the design mentioned above is as follows:

Table 6A.7 Statistical analysis of design for % Drug entrapment

Source	Sequential p-value	Lack of Fit p-value	Adjusted R ²	Predicted R ²	
Linear	0.0003	0.0006	0.7050	0.6095	
2FI	0.9809	0.0003	0.6230	0.2517	
Quadratic	< 0.0001	0.1055	0.9841	0.9134	Suggested
Cubic	0.1055		0.9931		Aliased

As shown in Table 6A.7, the best model to fit the experimental results of drug entrapment in nano-lipid constructs is the quadratic model and was chosen for further evaluation.

B) ANOVA Analysis for % Drug entrapment

The ANOVA for % Drug entrapment is given in table 6A.8.

Table 6A.8 ANOVA for Response Surface Quadratic Model for % Drug entrapment

Source	Sum of Squares	df	Mean Square	F-value	p-value	
Model	795.44	9	88.38	110.72	< 0.0001	significant
A-Lipid concentration	551.45	1	551.45	690.80	< 0.0001	
B-Surfactant concentration	1.60	1	1.60	2.01	0.1995	
C-Homogenization cycle	55.97	1	55.97	70.11	< 0.0001	
AB	0.8190	1	0.8190	1.03	0.3448	
AC	2.39	1	2.39	2.99	0.1274	
BC	0.0462	1	0.0462	0.0579	0.8167	

Chapter 6A) Formulation Development: DPK-060 Nano-lipid Constructs

A ²	151.84	1	151.84	190.22	< 0.0001	
B ²	6.12	1	6.12	7.66	0.0278	
C ²	14.49	1	14.49	18.15	0.0037	
Residual	5.59	7	0.7983			
Lack of Fit	4.20	3	1.40	4.04	0.1055	not significant
Pure Error	1.39	4	0.3468			
Cor Total	801.03	16				

The Model F-value of 110.72 implies the model is significant. In this case, A, C, A², B², C² are significant model terms. The Lack of Fit F-value of 4.04 implies the Lack of Fit is not significant relative to the pure error. The value of ANOVA shows that the effects of factors were significant; hence, the model is significant for % drug entrapment. From ANOVA table 6A.8, we can observe that F value was high for Factor A (690.80) and Factor C (70.11) than Factor B (2.01), it indicates that all the factors affect the % drug entrapment, which can also be observed visually from the surface plots (contour plots and 3D plots). Among the variables affecting % drug entrapment, lipid concentration and homogenization cycles have maximum effect on % drug entrapment. In addition, the actual v/s predicted plot for % drug entrapment shows an R² of 0.9930 which is a good correlation (Fig. 6A.2).

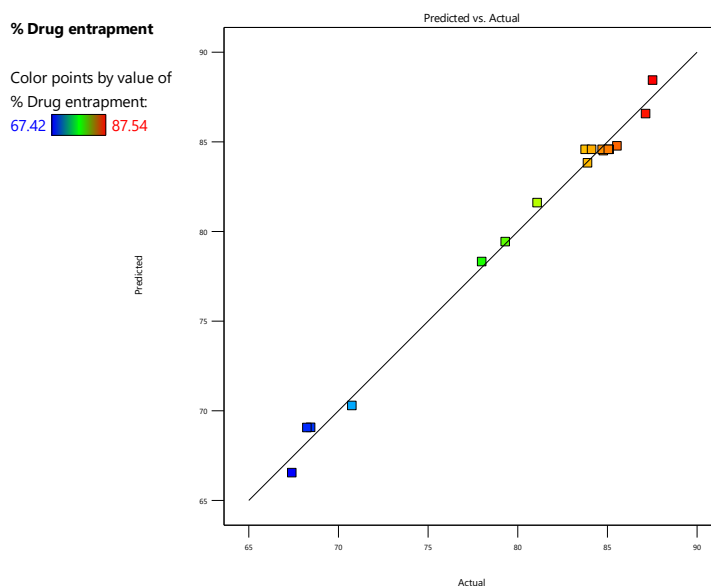


Figure 6A.2 Actual v/s Predicted plot for % Drug entrapment

Table 6A.9 ANOVA study results for % Drug entrapment

Parameters	Results of Response
Std Deviation	0.8935
Mean	80.30
C.V.%	1.11
R-Squared	0.9930
Adjusted R-Squared	0.9841
Predicted R-Squared	0.9134
Adeq. Precision	31.9516

C) Mathematical Model for % Drug entrapment

To evaluate the effect of various factors on % drug entrapment, contour plots and the 3D plot were referred to along with the value of ANOVA. From Table 6A.8, we can observe that with change in the combination of various factors, the final response, i.e., % drug entrapment, confirms the effect of multiple factors. Looking closely at different factor involved provide us a better understanding of the extent of the impact. The equation talks about the type of effect that is positive or negative.

Final equation in terms of coded factors:

$$\% \text{ Drug entrapment} = 84.568 + 8.3025 * A + 0.4475 * B - 2.645 * C + 0.4525 * AB - 0.7725 * AC + 0.1075 * BC - 6.00525 * A^2 - 1.20525 * B^2 - 1.85525 * C^2$$

Final Equation in Terms of Actual Factors

% Drug entrapment	=
-54.70300	
+56.98450	Lipid concentration
+0.648700	Surfactant concentration
-1.53020	Homogenization cycle
+0.090500	Lipid concentration * Surfactant concentration
-0.154500	Lipid concentration * Homogenization cycle

Chapter 6A) Formulation Development: DPK-060 Nano-lipid Constructs

+0.004300	Surfactant concentration * Homogenization cycle
-6.00525	Lipid concentration ²
-0.048210	Surfactant concentration ²
-0.074210	Homogenization cycle ²

The data demonstrates the higher F value for Factor A (690.80) and Factor C (70.11), i.e., lipid concentration and homogenization cycles have maximum effect on % drug entrapment. There was an increase in % drug entrapment with an increase in lipid concentration, which may be due to the partitioning of DPK 060 into the lipodic phase [13]. While the decrease in % drug entrapment was observed with an increase in homogenization cycles to some extent. Whereas, increase in % drug entrapment was observed with an increase in surfactant concentration to some extent. Surfactant may favour the stabilization of particles and encapsulation of drug into the nanoparticles [14]. Fig. 6A.3-6A.8 demonstrates the effects of independent variables on the % drug entrapment. The red area shows the maximum % drug entrapment, and the blue zone represents the area with the lowest % drug entrapment.

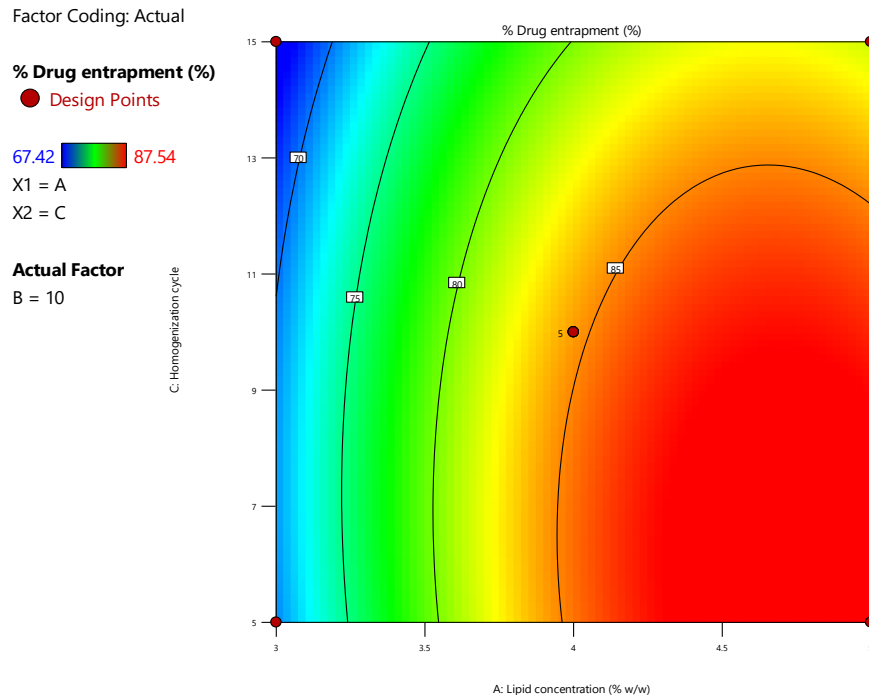


Figure 6A.3 Contour plot (2D) showing the combined effect of lipid concentration and homogenization cycles on % drug entrapment

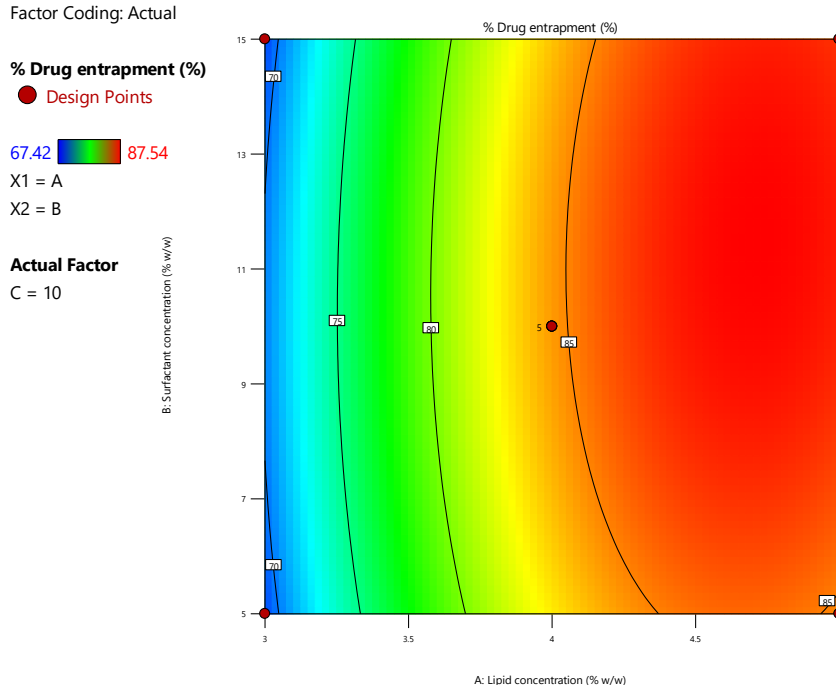


Figure 6A.4 Contour plot (2D) showing the combined effect of lipid concentration and Surfactant concentration on % drug entrapment

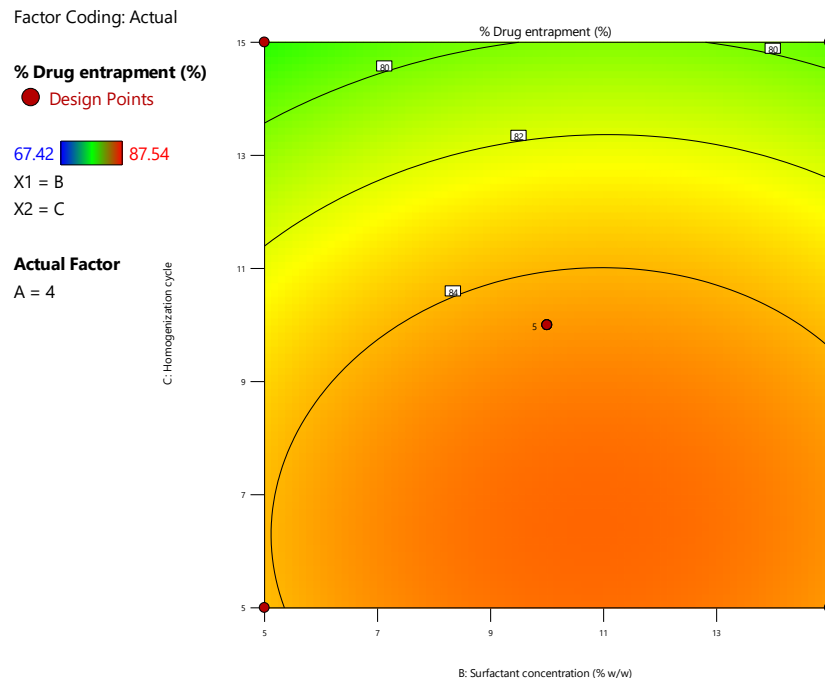


Figure 6A.5 Contour plot (2D) showing the combined effect of Surfactant concentration and Homogenization cycles on % drug entrapment

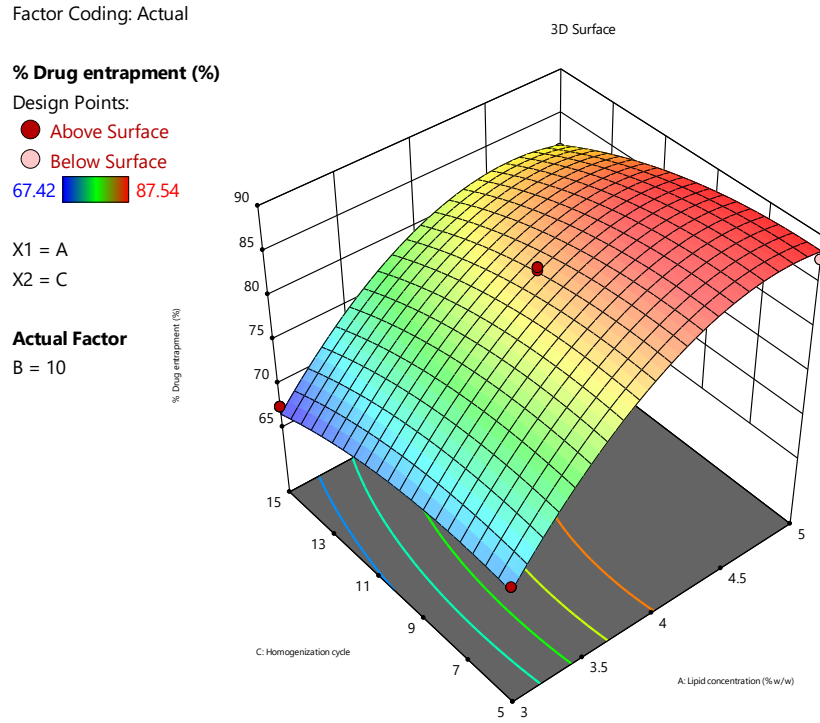


Figure 6A.6 Response surface (3D) showing the combined effect of lipid concentration and Homogenization cycles on % drug entrapment

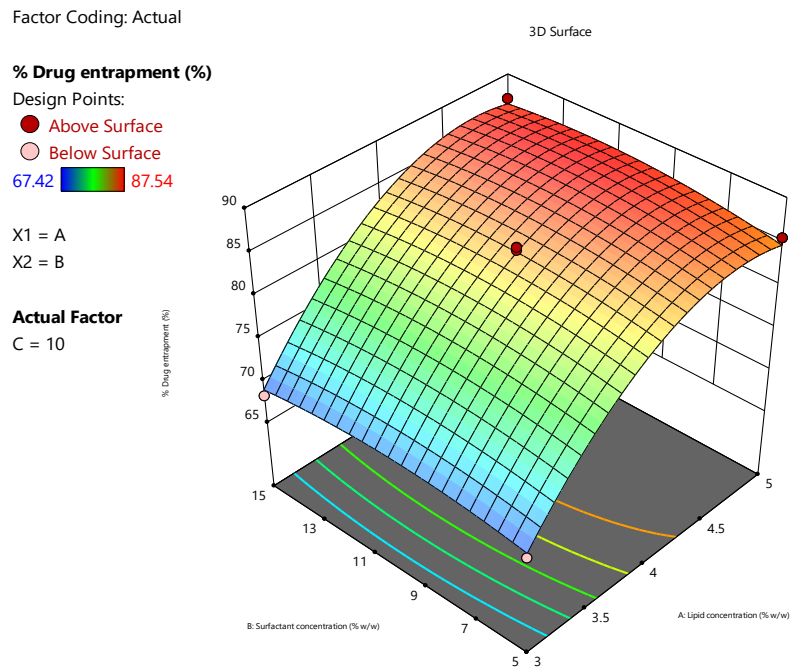


Figure 6A.7 Response surface (3D) showing the combined effect of lipid concentration and Surfactant concentration on % drug entrapment

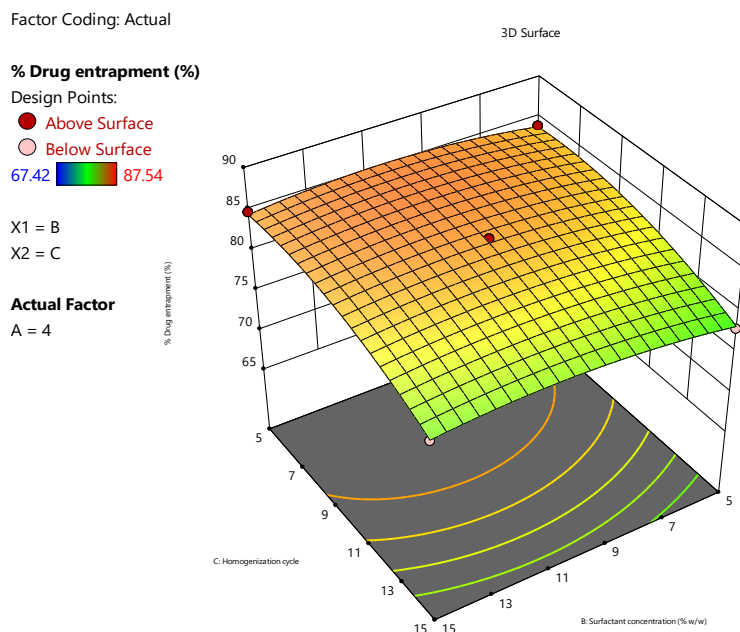


Figure 6A.8 Response surface (3D) showing the combined effect of Surfactant concentration and Homogenization cycles on % drug entrapment

6A.4.1.3.2 Influence of investigated parameters on Particle size

A) Statistical Analysis for Particle size

The statistical analysis of the design mentioned above is as follows:

Table 6A.10 Statistical analysis of design for Particle size

Source	Sequential p-value	Lack of Fit p-value	Adjusted R ²	Predicted R ²	
Linear	0.0051	0.0005	0.5255	0.3252	
2FI	0.9439	0.0002	0.4052	-0.3603	
Quadratic	< 0.0001	0.1213	0.9795	0.8911	Suggested
Cubic	0.1213		0.9904		Aliased

As shown in Table 6A.10, the best model to fit the experimental results of Particle size in NLCs is the quadratic model and was chosen for further evaluation.

B) ANOVA Analysis for Particle size

The ANOVA for Particle size is given in Table 6A.11.

Table 6A.11 ANOVA for Response Surface Quadratic Model for Particle size

Source	Sum of Squares	df	Mean Square	F-value	p-value	
Model	9663.58	9	1073.73	85.93	< 0.0001	significant
A-Lipid concentration	4204.44	1	4204.44	336.48	< 0.0001	
B-Surfactant concentration	99.41	1	99.41	7.96	0.0258	
C-Homogenization cycle	1687.80	1	1687.80	135.08	< 0.0001	
AB	9.00	1	9.00	0.7203	0.4241	
AC	125.44	1	125.44	10.04	0.0157	
BC	0.2500	1	0.2500	0.0200	0.8915	
A ²	3284.57	1	3284.57	262.86	< 0.0001	
B ²	1.95	1	1.95	0.1558	0.7048	
C ²	143.11	1	143.11	11.45	0.0117	
Residual	87.47	7	12.50			
Lack of Fit	64.10	3	21.37	3.66	0.1213	not significant
Pure Error	23.37	4	5.84			
Cor Total	9751.04	16				

The Model F-value of 85.93 implies the model is significant. In this case, A, B, C, AC, A², C² are significant model terms. The Lack of Fit F-value of 3.66 implies the Lack of Fit is not significant relative to the pure error. The value of ANOVA shows that the effects of factors were significant; hence, the model is significant for % Particle size. From ANOVA Table 6A.11, we can observe that F value was high for Factor A (336.48) and Factor C (135.08) than Factor B (7.96), it indicates that all the factors affect the particle size to some extent which can also be observed visually from the surface plots

Chapter 6A) Formulation Development: DPK-060 Nano-lipid Constructs

(contour plots and 3D plots). Among the variables affecting particle size, lipid concentration and homogenization cycles have maximum effect on particle size. In addition, the actual v/s predicted plot for Particle size shows an R^2 of 0.9910 which is a good correlation (Fig. 6A.9).

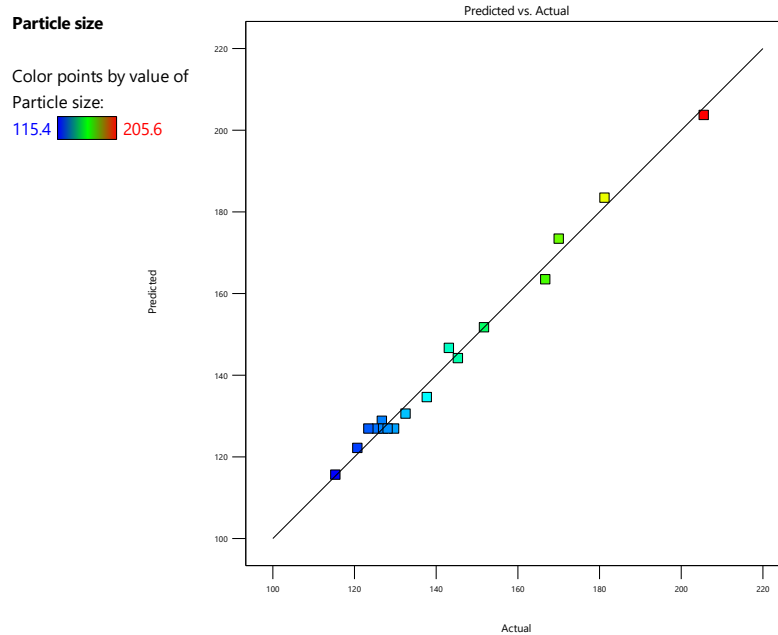


Figure 6A.9 Actual v/s Predicted plot for Particle size

Table 6A.12 ANOVA study results for Particle size

Parameters	Results of Response
Std. Deviation	3.53
Mean	143.05
C.V.%	2.47
R-Squared	0.9910
Adjusted R-Squared	0.9795
Predicted R-Squared	0.8911
Adeq. Precision	32.4958

C) Mathematical Model for Particle Size

To assess the effect of various factors on Particle size, contour plots and 3D plots were referred to along with the value of ANOVA. From Table 6A.11, we can observe

Chapter 6A) Formulation Development: DPK-060 Nano-lipid Constructs

that with change in the combination of various levels of factors, the final response, i.e., particle size confirming the effect of various factors. Looking closely at different factor involved provide us a better understanding of the extent of the impact. The equation talks about the type of effect that is positive or negative.

The final equation in terms of coded factors:

$$\text{Particle size} = 126.84 + 22.925 * A - 3.525 * B - 14.525 * C - 1.5 * AB - 5.6 * AC + 0.25 * BC + 27.93 * A^2 + 0.68 * B^2 + 5.83 * C^2$$

The final equation in terms of Actual factors:

Particle size	=
+488.36000	
-186.31500	Lipid concentration
-0.149000	Surfactant concentration
-3.18900	Homogenization cycle
-0.300000	Lipid concentration * Surfactant concentration
-1.12000	Lipid concentration * Homogenization cycle
+0.010000	Surfactant concentration * Homogenization cycle
+27.93000	Lipid concentration ²
+0.027200	Surfactant concentration ²
+0.233200	Homogenization cycle ²

The data demonstrates the higher F value for Factor A (336.48) and Factor C (135.08), i.e., lipid concentration and homogenization cycles have maximum effect on particle size. The increase in particle size was observed with increased lipid concentration. The viscosity of the dispersed phase (melted lipidic phase) will increase with an increase in lipid concentration and thus increase the size of the dispersion, which may be the possible reason for the increase in the particle size. While, the increase in homogenization cycles reduces particle size as previously reported [13, 15]. Fig. 6A.10-6A.15 demonstrates the effects of independent variables on particle size. The red area shows maximum particle size and blue zone represents the area with the lowest particle size.

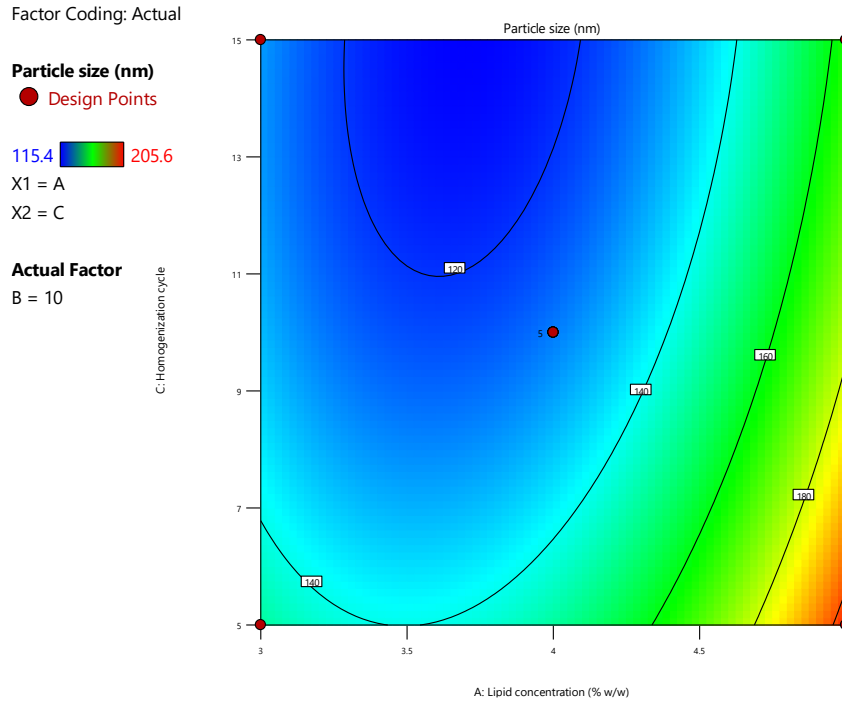


Figure 6A.10 Contour plot (2D) showing the combined effect of lipid concentration and Homogenization cycles on Particle size

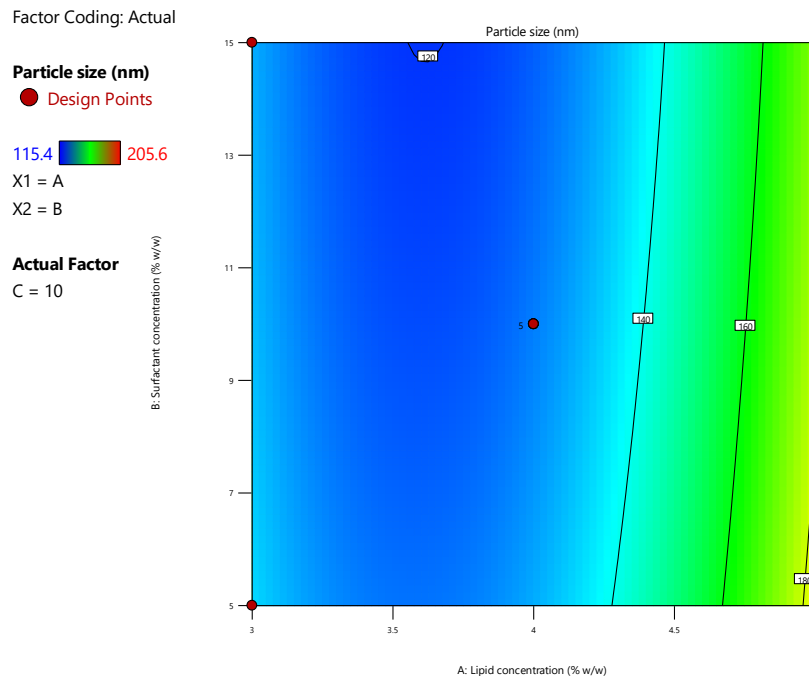


Figure 6A.11 Contour plot (2D) showing the combined effect of lipid concentration and Surfactant concentration on Particle size

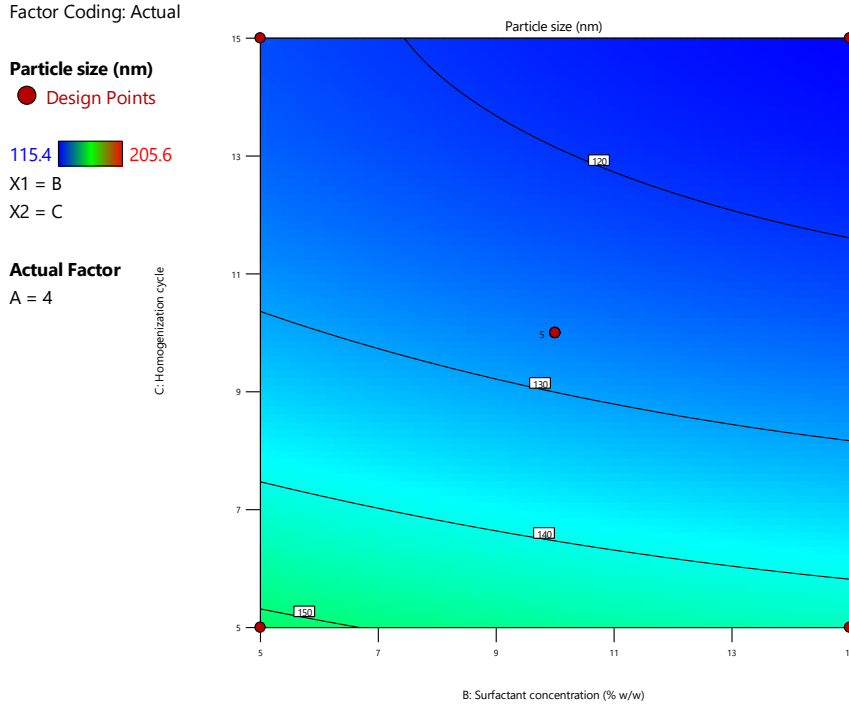


Figure 6A.12 Contour plot (2D) showing the combined effect of Surfactant concentration and Homogenization cycles on Particle size

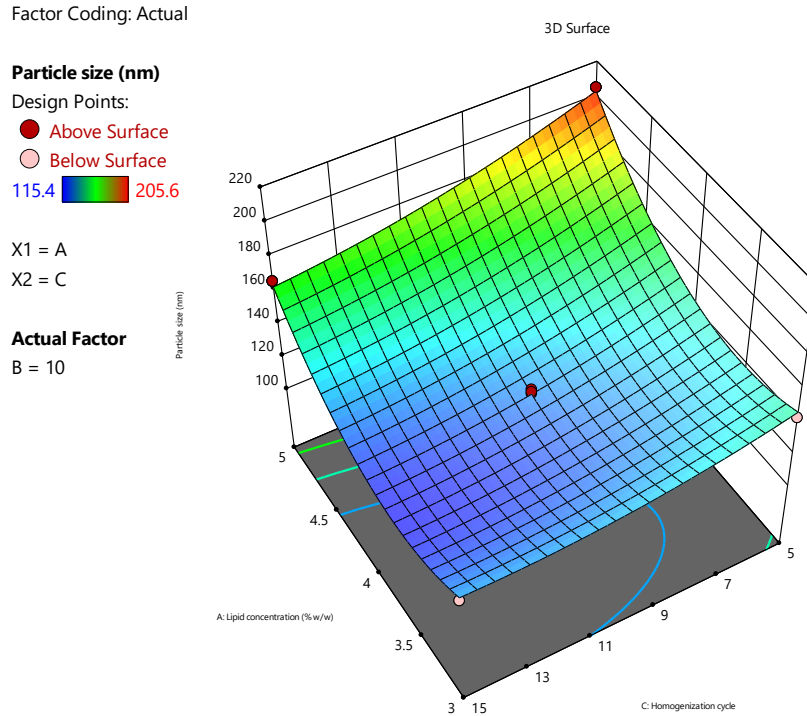


Figure 6A.13 Response surface (3D) showing the combined effect of lipid concentration and Homogenization cycles on Particle size

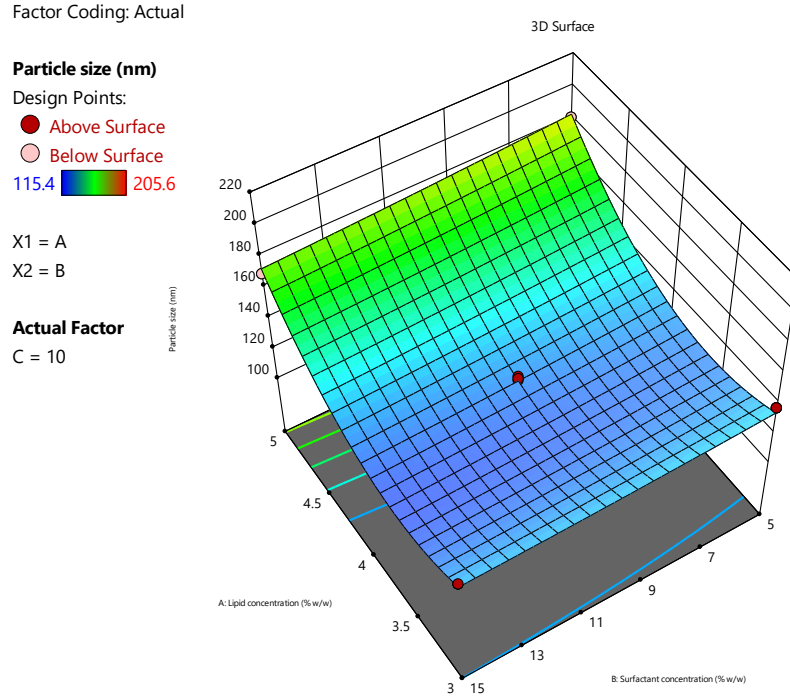


Figure 6A.14 Response surface (3D) showing the combined effect of lipid concentration and Surfactant concentration on Particle size

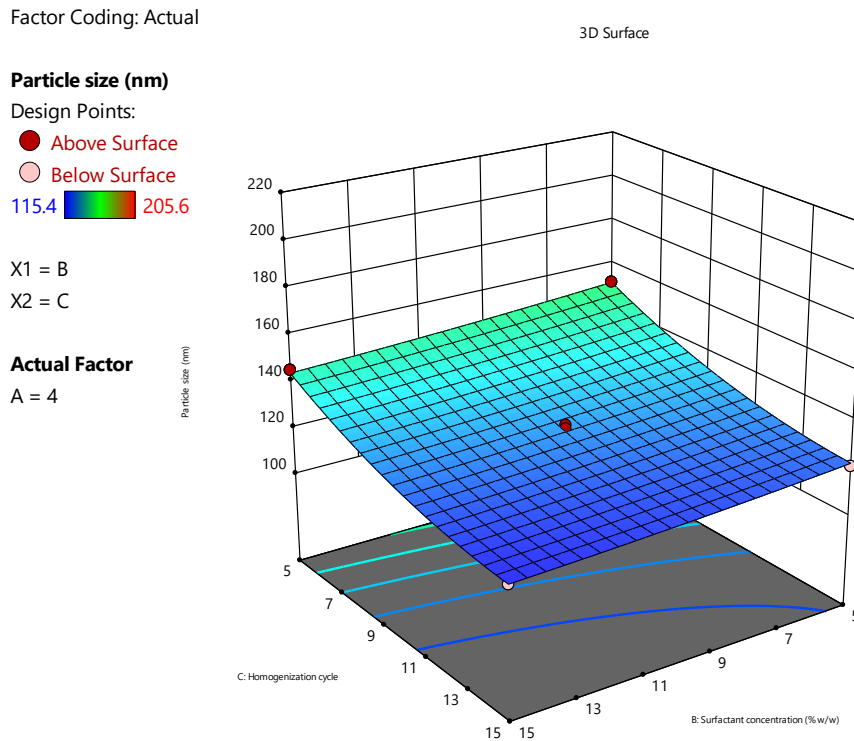


Figure 6A.15 Response surface (3D) showing the combined effect of Surfactant concentration and Homogenization cycles on Particle size

6A.4.1.3.3 Optimization using Desirability plot

A desirability plot gives the optimum value of variables to get desired responses. A desirability plot was generated (Fig. 6A.16) using Design Expert 13.0. Parameters for the desirability batch are shown in Table 6A.13 and the evaluation of the desirability batch in Table 6A.14.

Table 6A.13 Variables for desirability plot and goals for response

Name	Goal	Lower Limit	Upper Limit
A: Lipid concentration (% w/w)	In range	2	4
B: Surfactant concentration (% w/w)	In range	5	15
C: Homogenization cycles (No.)	target	10	
% Drug entrapment (%)	Maximize	67.42	87.54
Particle size (nm)	Minimize	100	150

Chapter 6A) Formulation Development: DPK-060 Nano-lipid Constructs

Factor Coding: Actual

All Responses

● Design Points

0.000 1.000

X1 = A

X2 = B

Actual Factor

C = 10

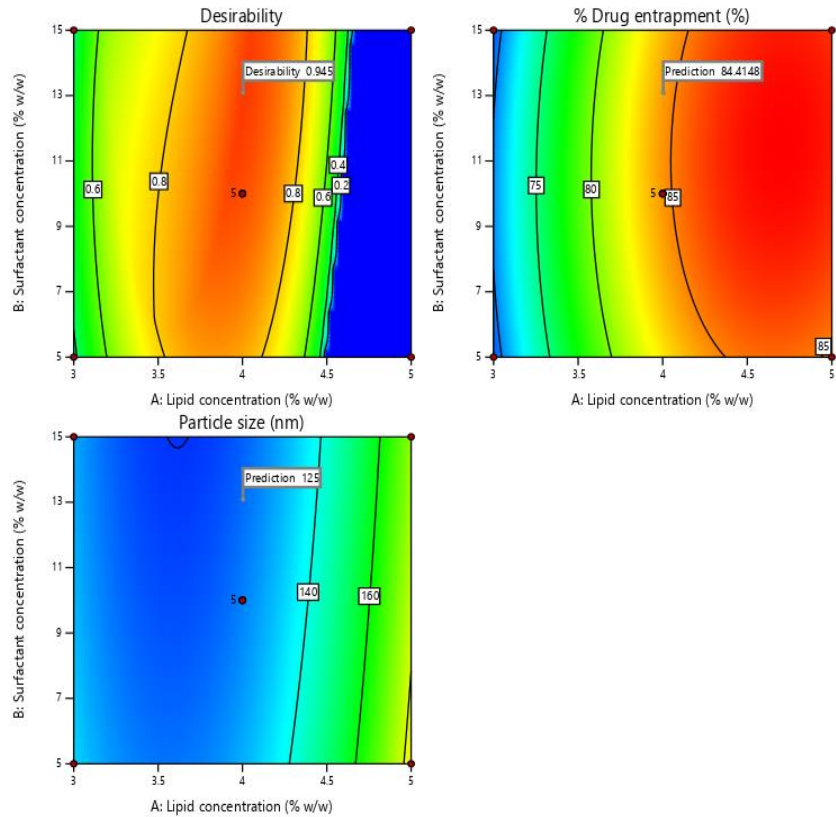


Figure 6A.16 Desirability plot

Table 6A.14 Desirability Plot for Optimization solution for DPK-060 nano-lipid constructs

Exp. Run	Lipid concentration (%w/w)	Surfactant concentration (%w/w)	Homogenization cycles (No.)	% Drug entrapment	Particle size (nm)	Desirability
1	4.004	13.088	10	84.415	125.0	0.945

Table 6A.15 Results of Evaluation of desirability batch

Response	Experimental value	Predicted value	Residual Difference
% Drug entrapment	85.20	84.415	0.78
Particle size (nm)	128.6	125.0	3.6

The obtained results demonstrate the suitability of the predicted desirability plot of the optimized NLC formulation.

6A.4.1.3.4 Establishment of Design Space

ICH Q8 (2008) defines “Design Space” as a “multidimensional combination and interaction input variables and process parameters that have been established to provide assurance of quality.” The composite desirability function based on the set constraints was used to determine the conditions that would result in an optima formulation design.

6A.4.1.3.5 Overlay Plot for predicted design space

The experimental design was used for multiple responses: % Drug entrapment and particle size. Overlay plot (Fig. 6A.17) can be obtained by superimposing contour plots of both responses, which displays possible response values in the factor space. The region highlighted in yellow is where a slight variation in the critical variables won't affect the final response and the response will be in the desired range. Areas that do not fit the optimization criteria are shaded gray, while design space is accepted colored yellow. Fig. 6A.17 shows an overlay plot based on the desirability criteria.

Chapter 6A) Formulation Development: DPK-060 Nano-lipid Constructs

Factor Coding: Actual

Overlay Plot

% Drug entrapment

Particle size

● Design Points

X1 = A

X2 = B

Actual Factor

C = 10

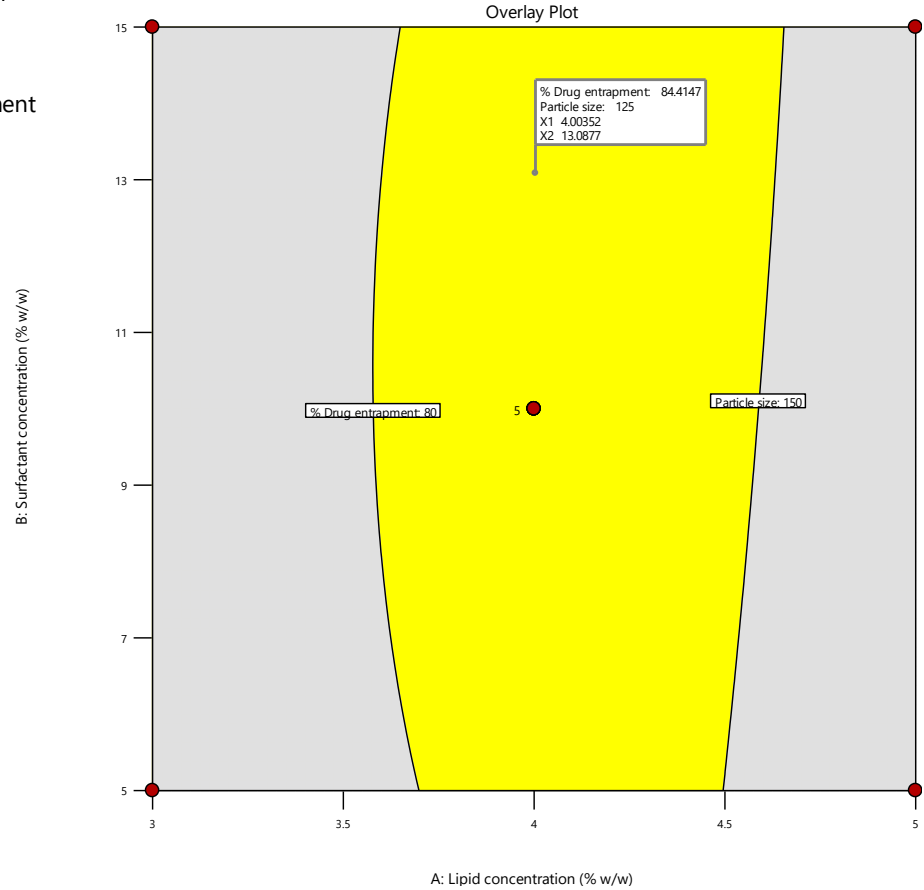


Figure 6A.17 Overlay plot

Table 6A.16 Composition of optimized batch of DPK-060 NLCs and gel

Formulation components	Concentration
DPK-060/DPK-060 NLCs	1% w/v
Lipid concentration	3.133 % w/w
Surfactant concentration	10 % w/w
Homogenization cycles	1000 psi * 10 cycles
Carbopol 934P	1.20% w/v
Propylene glycol	4% w/v
Methyl paraben	0.2 % w/v
Propyl paraben	and 0.02 % w/v
Sodium hydroxide solution (10% v/v)	...qs...to pH 6.5

6A.4.2 Characterization of optimized DPK-060 NLCs and DPK-060 NLC gel

6A.4.2.1 Zeta potential

The zeta potential graph of optimized DPK-060 NLCs (Fig. 6A.18) showed a net negative charge of NLCs with a Z-avg value of -22.5 mV. The charge was found sufficient enough to keep the particles dispersed via repulsive forces.

6A.4.2.2 Shape and surface morphology

Scanning electron microscopy of optimized DPK-060 nano-lipid constructs was performed, and the image is represented as Fig. 6A.19. The image showed the spherical shape of NLCs. The size of nano-lipid constructs seen in the image was found in line with the results of particle size data obtained from the Malvern zeta sizer (Fig. 6A.20).

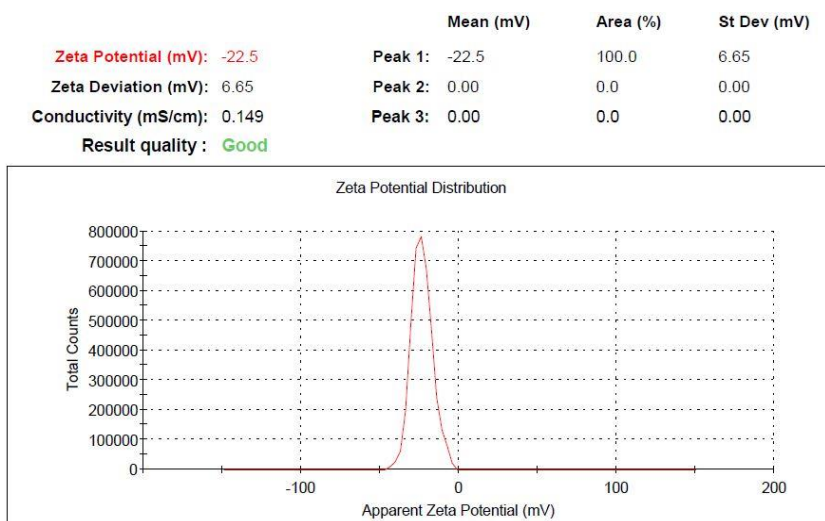


Figure 6A.18 Zeta potential of the developed DPK-060 nano-lipid constructs

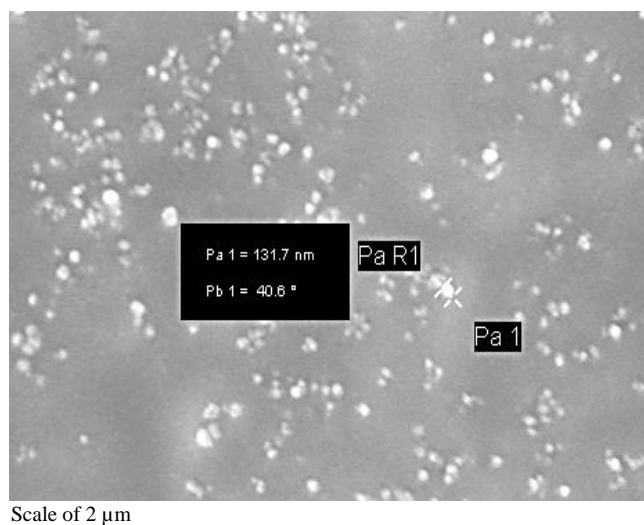


Figure 6A.19 SEM image of the developed DPK-060 loaded nano-lipid constructs

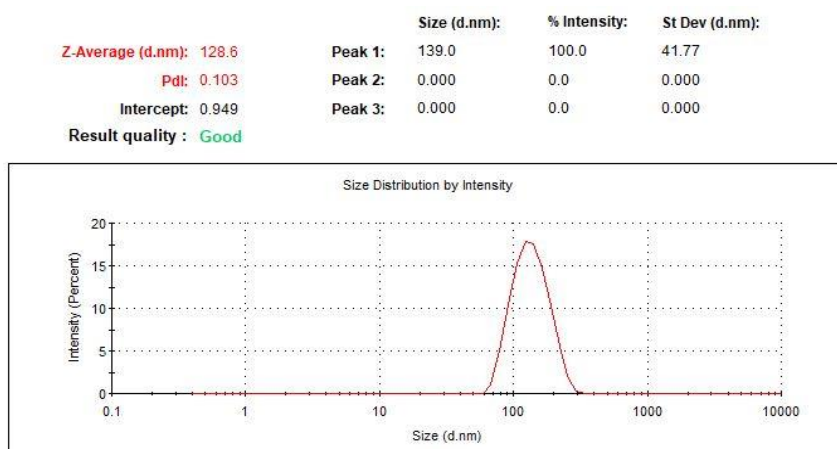


Figure 6A.20 Particle size of the optimized DPK-060 nano-lipid constructs

6A.4.2.3 % Drug entrapment and % drug loading

% Drug entrapment and % drug loading of the optimized DPK-060 nano-lipid constructs were found to be 85.34 ± 1.05 % and 6.7 ± 0.4 % w/w, respectively.

6A.4.2.4 Viscosity of DPK-060 NLC gel

The viscosity of free DPK-060 gel and DPK-060 NLC gel was found to be 13.10 ± 0.292 Pa.S and 16.22 ± 0.451 Pa.S, respectively.

6A.4.2.5 Spreadability of DPK-060 NLC gel

The spreadability of free DPK-060 gel and DPK-060 NLC gel was 6.87 ± 2.07 cm² and 7.69 ± 1.38 cm², respectively. The spreadability of free DPK-060 gel was lesser than DPK-060 NLC gel which may be attributed to the increased solid content of the gel after the addition of NLC formulation.

6A.4.2.6 pH of DPK-060 NLC gel

The pH of free DPK-060 gel and DPK-060 NLC gel was found to be 6.4 ± 0.4 and 6.5 ± 0.4 , respectively.

6A.4.2.7 Assay of DPK-060 gel

The DPK-060 content in free DPK-060 gel and DPK-060 NLC gel was found to be 99.58 ± 1.25 % and 99.05 ± 1.62 %, respectively.

6A.5 References

1. Sharma, G., et al., *Nanostructured lipid carriers: a new paradigm in topical delivery for dermal and transdermal applications*. Critical Reviews™ in Therapeutic Drug Carrier Systems, 2017. **34**(4).
2. Souto, E.B., et al., *SLN and NLC for topical, dermal, and transdermal drug delivery*. Expert opinion on drug delivery, 2020. **17**(3): p. 357-377.
3. Garcês, A., et al., *Formulations based on solid lipid nanoparticles (SLN) and nanostructured lipid carriers (NLC) for cutaneous use: A review*. European Journal of Pharmaceutical Sciences, 2018. **112**: p. 159-167.
4. Rehman, S., et al., *Tailoring lipid nanoconstructs for the oral delivery of paliperidone: Formulation, optimization and in vitro evaluation*. Chemistry and Physics of Lipids, 2021. **234**: p. 105005.
5. Carvajal-Vidal, P., et al., *Development of Halobetasol-loaded nanostructured lipid carrier for dermal administration: Optimization, physicochemical and biopharmaceutical behavior, and therapeutic efficacy*. Nanomedicine: Nanotechnology, Biology and Medicine, 2019. **20**: p. 102026.

6. Qumber, M., et al., *BBD-based development of itraconazole loaded nanostructured lipid carrier for topical delivery: in vitro evaluation and antimicrobial assessment*. Journal of Pharmaceutical Innovation, 2020: p. 1-14.
7. Rathod, V.R., D.A. Shah, and R.H. Dave, *Systematic implementation of quality-by-design (QbD) to develop NSAID-loaded nanostructured lipid carriers for ocular application: preformulation screening studies and statistical hybrid-design for optimization of variables*. Drug development and industrial pharmacy, 2020. **46**(3): p. 443-455.
8. Lawrence, X.Y., *Pharmaceutical quality by design: product and process development, understanding, and control*. Pharmaceutical research, 2008. **25**(4): p. 781-791.
9. Porfire, A., et al., *Pharmaceutical development of liposomes using the QbD approach*. Liposomes Adv. Perspect, 2019. **2019**: p. 1-20.
10. Mitra, S., et al., *Tumour targeted delivery of encapsulated dextran–doxorubicin conjugate using chitosan nanoparticles as carrier*. Journal of Controlled Release, 2001. **74**(1): p. 317-323.
11. Batheja, P., et al., *Topical drug delivery by a polymeric nanosphere gel: formulation optimization and in vitro and in vivo skin distribution studies*. Journal of controlled release, 2011. **149**(2): p. 159-167.
12. Shah, K.A., et al., *Solid lipid nanoparticles (SLN) of tretinoin: potential in topical delivery*. International journal of pharmaceutics, 2007. **345**(1-2): p. 163-171.
13. Nagaich, U. and N. Gulati, *Nanostructured lipid carriers (NLC) based controlled release topical gel of clobetasol propionate: design and in vivo characterization*. Drug delivery and translational research, 2016. **6**(3): p. 289-298.
14. Chauhan, I., et al., *Nanostructured lipid carriers: A groundbreaking approach for transdermal drug delivery*. Advanced pharmaceutical bulletin, 2020. **10**(2): p. 150.
15. Qumber, M., et al., *BBD-based development of itraconazole loaded nanostructured lipid carrier for topical delivery: in vitro evaluation and antimicrobial assessment*. Journal of pharmaceutical innovation, 2021. **16**(1): p. 85-98.